

## DEVELOPMENT OF A PYTHON-BASED STOREY LOSS FUNCTION GENERATOR

Davit Shahnazaryan<sup>1</sup>, Gerard J. O'Reilly<sup>1</sup>, and Ricardo Monteiro<sup>1</sup>

<sup>1</sup>Centre for Training and Research on Reduction of Seismic Risk (ROSE), Scuola Universitaria  
Superiore IUSS Pavia  
Palazzo del Broletto, Piazza della Vittoria 15, Pavia 27100, Italy  
e-mail: {davit.shahnazaryan,gerard.oreilly,ricardo.monteiro}@iusspavia.it

---

### Abstract

*With the development of performance-based earthquake engineering (PBEE) for mitigating seismic risk, significant work has been carried out to implement risk-based design and assessment frameworks. However, the probabilistic nature and computationally heavy implementation of the PBEE framework when using a component-based loss assessment approach, made it less desirable for practitioners. As a consequence, methods employing storey loss functions (SLFs), which ease the computational cost of the component-based approach, have emerged. The use of predefined SLFs, especially at a design stage, is desirable where component information is likely missing. This article describes an object-oriented toolbox, recently developed in Python, for the estimation of SLFs. The step-by-step implementation is described along with a comparative demonstration of its application to a case study existing building versus the more rigorous component-based approach described in FEMA P-58. The attained loss metrics demonstrate the quality and prove that the SLF-based approach, while being more simplistic in nature, achieves accurate results with relative ease across all levels of seismic response.*

**Keywords:** PBEE, seismic assessment, loss estimation, storey loss function.

---

## 1 INTRODUCTION

Over the years, it has become paramount to characterize seismic risk using terms more meaningful to stakeholders and practitioners. These performance measures can be characterised by losses, downtime and casualties/fatalities. To avoid describing performance at discrete hazard levels, as typically prescribed in design codes (e.g. [1]–[3]), probabilistic frameworks have been developed to include uncertainties for hazard, structural response, damage and monetary loss. One of these frameworks is the performance-based earthquake engineering (PBEE) proposed by the Pacific Earthquake Engineering Research (PEER) Center [4]. However, due to its probabilistic nature and computationally expensive implementation, it has become popular primarily within academic research or specialized reports, such as FEMA P-58 [5], rather than a widespread code-based implementation for practitioners. While existing structures might offer easily-accessible information regarding their component inventory, the opposite is the case for newly designed structures and practitioners may be hesitant to carry out a full loss-driven design consisting of many trials and iterations. Over the years, many risk-targeted design methods have been developed, where many of them ([6]–[13]) are risk-targeted approaches using collapse risk as their primary design objective, while others ([9], [11], [14]) explore the possibility of using economic loss as well. To simplify the codification of these approaches, alternatives to component-based probabilistic loss estimation are sought.

Ramirez and Miranda [15] looked into simplifying the PEER's building-specific loss estimation methodology by creating so-called engineering demand parameters versus decision variable (EDP-DV) functions, where the structural response parameters, or EDPs, are directly related to economic losses, or DVs. These functions typically define monetary loss at a storey level hence are termed storey loss functions (SLF). They provide readymade loss functions describing the repair costs over a predefined building inventory of damageable components in a simplified manner, thus reducing the amount of data required to be handled for the building's inventory during loss assessment. As mentioned earlier, during the design phase of new buildings, the complete component inventory of the building might not be fully known, therefore generic SLFs will potentially help avoid the issue of having excessive computations required in component-based driven approaches. These SLFs have been recently implemented in Silva *et al.* [16] for steel buildings in a European context, for example, although options for reinforced concrete (RC) buildings are generally lacking.

Based on the storey loss estimation framework by Ramirez and Miranda [15], a toolbox for creating generic user-based SLFs has been developed. Component quantities, fragility and consequence functions are used as input elements to generate FEMA P-58 compatible SLFs [5]. While the framework by Ramirez and Miranda [15] uses cost distributions for different RC building occupancies in California, Papadopoulos *et al.* [17] developed SLFs for steel buildings in Greece. Similarly, SLFs were developed for URM buildings by Ottonelli *et al.* [18] and masonry infill walls by other researchers [19]–[21]. Additionally, recent studies on loss estimation ([22], [23]) highlighted the need for developing SLFs to cover a wide range of building characteristics, such as its storey-wise functionality, typology of structure, and occupancy. Sullivan [23] presented a simplified loss assessment approach to calculate expected annual loss, EAL, however, a limitation was mentioned, whereby the knowledge of quantity, distribution, and characteristics of all damageable components within the building inventory might not always necessarily be readily available and, to address it, SLFs may be used. On the contrary, Perrone *et al.* [22] proposed a method for estimating the EAL of Italian RC buildings using suitable SLFs, further highlighting the need for developing simplified alternatives.

This paper describes the development of a toolbox that allows the automated production of SLFs through regression analysis using the results of random sampling of component damage

states and costs, including damage correlation among components. Contrary to past research, the aim is not to create generic readymade loss functions for a specific building category, but to develop a tool for any user to create their own functions, based on an existing database of components, such as FEMA P-58 or expert opinion, without being limited to existing SLF libraries. The framework implemented within the toolbox is described herein. The main decisions encompassing the use of the toolbox include: the building characterisation through the definition of component inventory, defined by component quantities, fragility and consequence functions; performance grouping of components based on EDP sensitivity; identification of possible interactions among different components; choosing the number of simulations for the sampling of damage states; and selecting a regression fitting type. The latter may be extended by adding more regression options. Finally, the framework is validated with a case-study application to a generic RC building, and the results are compared with a component-based loss assessment of the same building (Figure 1) following FEMA P-58.

## 2 STOREY LOSS FUNCTION ESTIMATION TOOLBOX

As previously mentioned, the framework implemented within the SLF estimation toolbox consists of the following steps:

1. Building characterisation;
2. Component inventory definition;
3. Component grouping;
4. Consideration of correlations between components;
5. Monte Carlo Simulation of damage states;
6. Repair cost computation;
7. Storey loss function fitting.

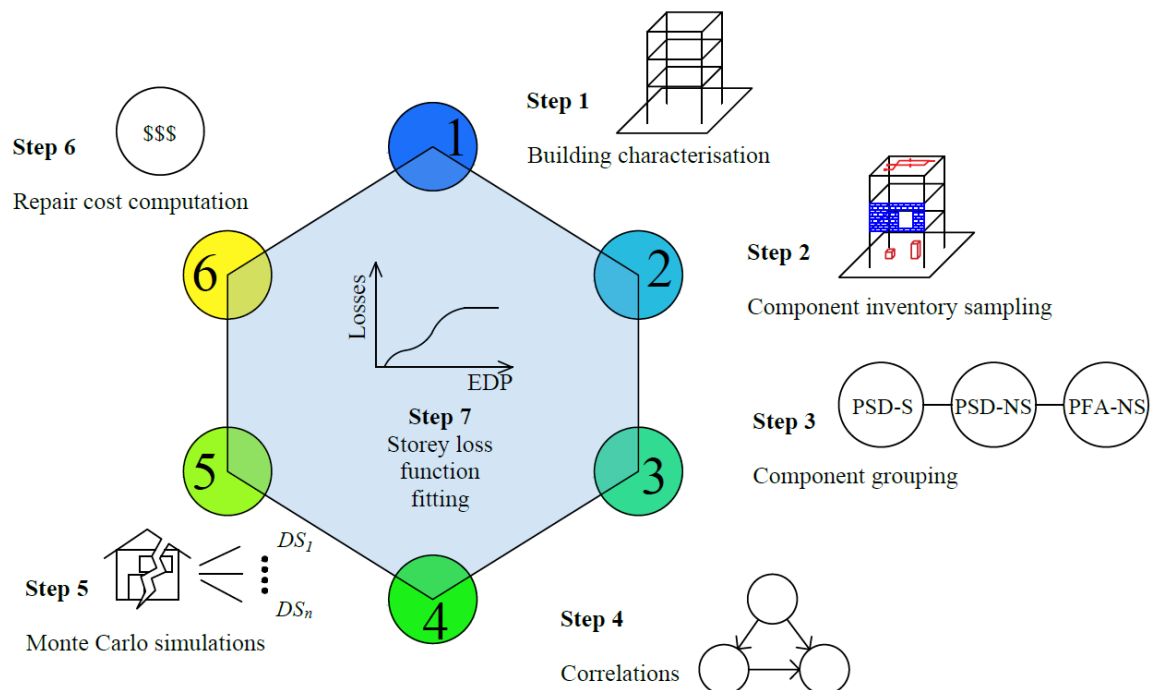


Figure 1: Flowchart of storey loss function generation framework.

The first step of the framework is the identification of the building's characteristics including the number of storeys, global dimensions, occupancy type and usage. However, if those are yet

to be identified, SLFs may still be identified for a desired reference area and extrapolated to a specific building configuration through the actual building area. Once the building characteristics have been identified, or the reference area selected, a damageable component inventory may be created. Building occupancy type and structural typology will play a key role in gaining insight into possible distributions of components if they are not preliminary known, as is common for new designs. The distributions (mean and uncertainty) of those components may be obtained from empirical and statistical data, collected from existing buildings and surveys, or based on expert opinion or personal judgment. The inventory consists of structural, non-structural components, and building contents likely to be damaged, all of which contribute to the economic losses deriving from required repair costs following seismic damage.

Typically, the component inventory has information on item types, component quantities, EDP sensitivity and typology (structural or non-structural) of each component. Three performance groups are identified unless otherwise specified, and fragility and consequence functions for the components should be provided. To compile the component database, damage states and associated fragility and consequence functions may be adapted from the FEMA P-58 database or other similar sources. Additionally, it needs to be specified whether the component will be affected by the EDP of the floor slab above the current storey or by the supporting floor slab at the current storey. For example, water distribution piping systems connected to the ceiling in a storey will be sensitive to the peak floor acceleration (PFA) of the above floor, while contents, such as electronic equipment will usually be sensitive to the PFA of the supporting floor. To account for this, a simplifying assumption is made within the toolbox, whereby the component losses in storey  $i$ , but affected by the upper floor, are computed as part of, or moved to, storey  $i+1$ . Even though the physical location of costs with respect to which storey the loss will be assigned is not quite correct, it will still lead to a correct total cost in the building.

In order to utilize the framework for 3D buildings, it needs to be applied to both directions of the building separately. Additionally, each direction will include components oriented along that direction. Essentially, the analyst would need to identify, for each damageable component at each storey level, in which principal direction of the building it is sensitive to damage. This way, the components can be grouped and analysed separately using the structural demands in the two orthogonal directions. To what pertains non-directional components, the framework is applied only once. In this case, both directions of seismic action are of importance, and the maximum value of two demand parameters in both directions may be multiplied by a non-directional conversion factor, as suggested in FEMA P-58, and used for a single SLF in the analysis. However, interactions of seismic effects in two orthogonal directions on a given component are not accounted for in cases where such interaction is expected to be significant, more advanced methods of loss assessment should be adopted.

Once the component inventory is identified, components may be classified into groups depending on the type of the component (i.e. structural or non-structural) and their EDP (e.g. peak storey drift (PSD) or PFA). Components within a performance group will be assessed together for a mutual demand and subsequent losses will be summed up to estimate the group's SLF. In other words, losses from all components within a performance group will be tied to the same EDP.

Similar to past studies ([15], [17]), the effects of such EDPs, such as vertical acceleration or building torsion, are not accounted for within the framework. Additionally, as discussed in O'Reilly *et al.* [24], torsion could be better dealt with by adopting a component-based approach. However, if one is to provide the toolbox with fragility and consequence functions associated with components other than PSD- or PFA-sensitive (e.g. peak floor velocity), the toolbox will still be capable of producing the appropriate SLFs. This classification of components into

different performance groups allows the disaggregation of losses at later stages to identify the main contributors to the economic losses, which can be useful in deciding which type of retrofitting strategies should be adopted as demonstrated by Carofilis *et al.* [25].

Similar to the studies of Ramirez and Miranda [15], structural and non-structural components sensitive to the same EDP may be grouped to allow for the consideration of possible correlations between the damage states. For example, a specific intensity level may not result in damage to a specific non-structural component, but it may affect a different component connected to it that does suffer a degree of damage. To repair this damaged component, access should be first granted, which foresees the removal of the portion or the entirety of the undamaged non-structural component. Essentially, for any independent component  $i$ , all damage states (DSs) are assumed to have an independent sequential occurrence unless otherwise specified and each DS is assumed to be mutually exclusive. A probability of occurrence is assigned to mutually exclusive DSs, which sum up to 100%. In contrast, if DS  $j$  of component  $i$  is dependent on the occurrence of a DS  $d$  of a component  $m$ , then the DS of component  $i$  is assumed independent of component  $m$  unless component  $m$  is in DS  $d$  or higher (i.e. DS  $d$  in component  $m$  triggers DS  $j$  in component  $i$ ). As illustrated in Figure 2, for an EDP of  $edp$ , if component  $m$  is in DS3, then even if there is no indication of damage for component  $i$ , the latter component is assumed to be in DS2.

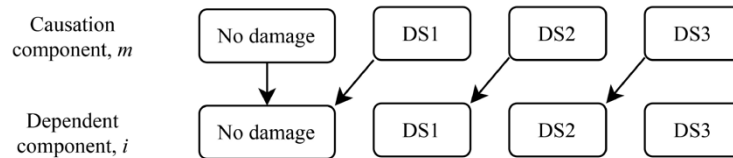


Figure 2: Relationship between causation and dependent components.

With a component inventory identified along with possible correlations among the damage states of different components, Monte Carlo simulations are performed. For each simulation, damage and repair costs are sampled for each component within the performance group, where all costs are added to obtain the performance group's total loss for a given EDP. Essentially, the algorithm samples damage states for each component at a given EDP level and for a specified number of simulations. A random value is generated within 0 and 1 and a DS is assigned to a component based on its fragility functions. An example describing the relationship between causation and dependent components is illustrated in Figure 3. At an EDP level of 0.02 (point 1 in Figure 3), if the sampled probability for the causation component is 0.3, then DS3 is assigned to the component. At the same EDP level, a sampled probability of 0.8 is assigned to the dependent component, which sets it in DS1. Following the relationship of the components described in Figure 2, the DS of the dependent component is modified to DS2.

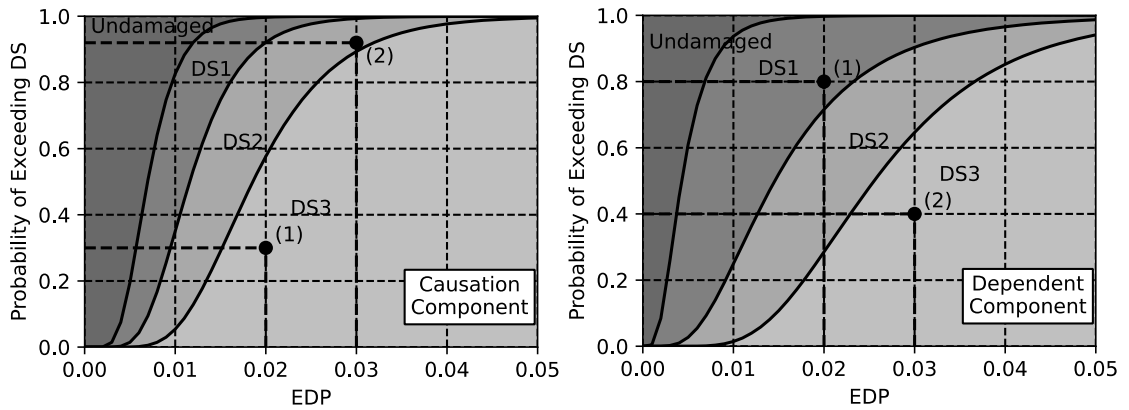


Figure 3: Damage states and fragility functions of a sample: (left) causation component and (right) dependent component.

Once damage states for all components have been sampled, repair costs may be evaluated. For each component, at each sampled DS, the repair cost is assigned based on the provided consequence function. If the consequence function is represented only by the mean value, then the mean value is assigned, while if a distribution is provided, then a value as the repair cost is sampled from the repair cost distribution.

Finally, SLFs for component groups may be identified through regression analysis on sampled repair costs. More than one analytical expression may be used within the toolbox at <https://github.com/davitshahnazaryan3/SLFGenerator> (Figure 4), while possible addition of new functions may be considered, as future research identifies better alternatives. The Weibull cumulative distribution function may be used to perform the regression, described in Equation 1:

$$y = \alpha \left( 1 - \exp \left( - \left( \frac{x}{\beta} \right)^\gamma \right) \right) \quad (1)$$

where,  $\alpha$ ,  $\beta$  and  $\gamma$  are the fitting coefficients,  $x$  is the EDP value and  $y$  is the fitted loss value. Alternatively, the regression model proposed by Papadopoulos *et al.* [17], defined in Equation 2, may be used:

$$y = \varepsilon \frac{x^\alpha}{\beta^\alpha + x^\alpha} + (1 - \varepsilon) \frac{x^\gamma}{\beta^\gamma + x^\gamma} \quad (2)$$

where,  $\alpha$ ,  $\beta$ ,  $\gamma$ ,  $\delta$  and  $\varepsilon$  are the fitting coefficients,  $x$  is the EDP value and  $y$  is the fitted loss value.

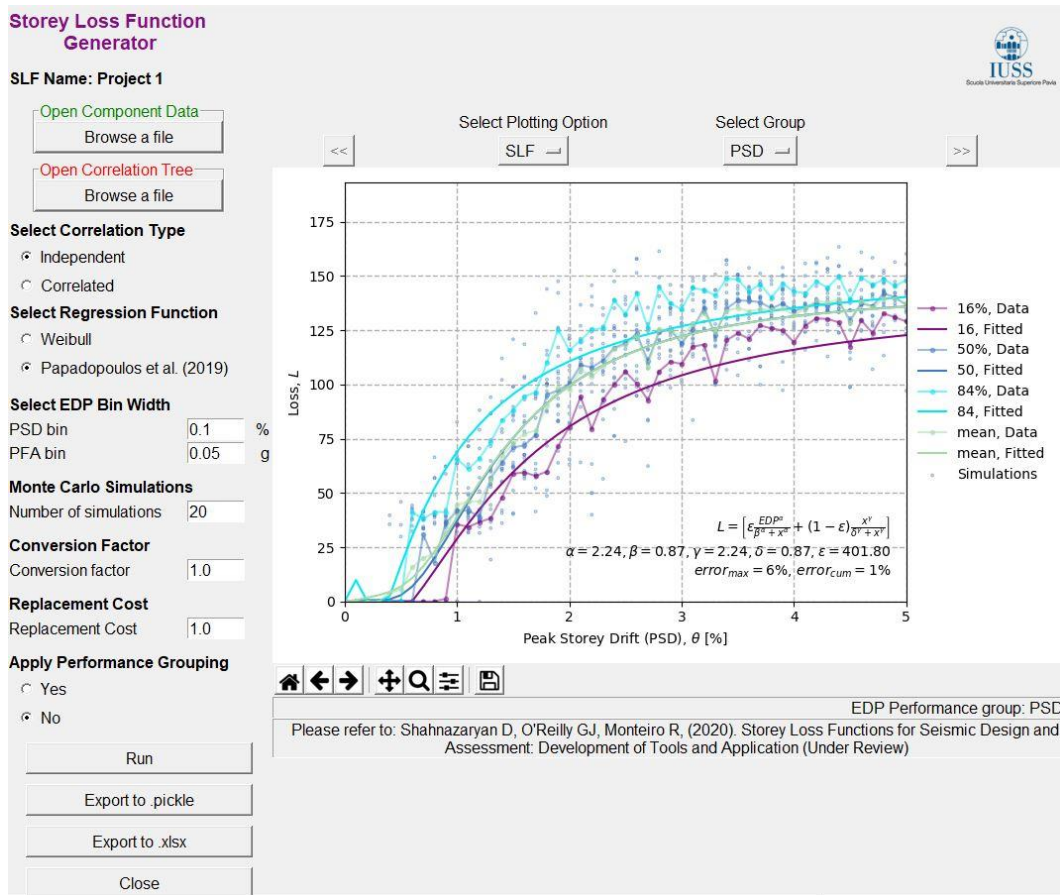


Figure 4: Overview of the storey loss function generator interface.

### 3 EXAMPLE APPLICATION

To demonstrate the capabilities of the toolbox for generating SLFs, a generic case-study RC building of 3 storeys and a reference area of 432 m<sup>2</sup> (Figure 5) is designed according to Eurocode 2 [26] and Eurocode 8, EC8, [27] provisions. Based on the design, a three-dimensional non-linear numerical model was created using OpenSees [28] and incremental dynamic analysis [29] was carried out. Finally, using the generated SLFs, loss assessment was carried out and compared with the component-based assessment following the FEMA P-58 guidelines. It is important to note that the results are not meant to be indicative of typical RC building performance, but more as a comparative exercise between the two approaches. The building is assumed to be located in the city of L'Aquila, Italy on a stiff clay site according to EC8's site classification. The gravity loads, including imposed and dead loads, were assumed as 8.06 kN/m<sup>2</sup> and 6.56 kN/m<sup>2</sup> at the general floor and roof level, respectively. The building has two seismic frames along its perimeter in each of the principal directions. The material properties used in the design and detailing were 25 MPa for the concrete compressive strength and 415 MPa for the steel yield strength. No plan or elevation irregularities are present.

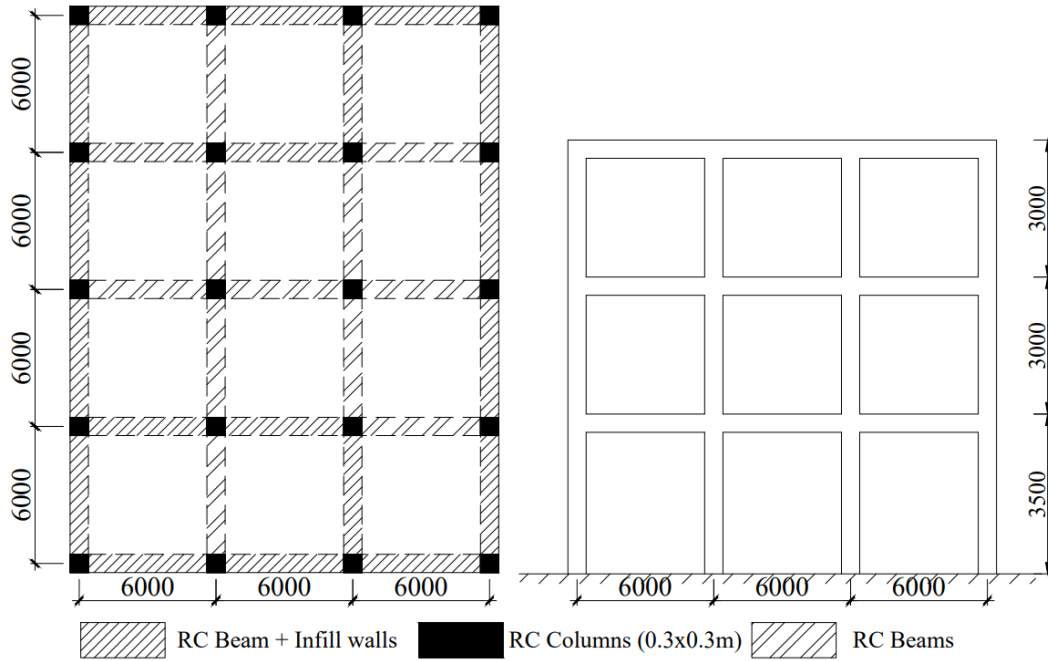


Figure 5: Plan and elevation view of the structural configuration of the case study building.

PFA and PSD sensitive components were considered within the component inventory of the case study building. Components with sensitivity towards one direction of seismic action and having the same EDP sensitivity were grouped, while non-directional components were classified into a different performance group. Moreover, PFA-sensitive components were grouped depending on the location within a storey and to which EDP they were sensitive. For example, components such as piping systems located in a storey  $j$  but sensitive to the EDP of the above storey were tied to the PFA of storey  $j+1$ , while electronic devices in storey  $j$  were tied to the PFA of storey  $j$ , as described previously. Table 1 to Table 3 summarise the mean structural, PSD-sensitive and PFA-sensitive non-structural component quantities.

Table 1: Mean quantities for the damageable PSD-sensitive non-structural components of the case-study RC building in X (Y) direction.

ID	Component	Unit	Quantity per storey		
			Storey 1	Storey 2	Storey 3
B101	Exterior masonry infill with windows	per m <sup>2</sup>	84(63)	72(54)	72(54)
B102	Internal masonry partition		67.75 (32.3)	59.8 (24.2)	59.8 (24.2)
B103	Internal gypsum partition		105(75)	95(62)	95(62)
B104	Non-monolithic precast concrete stairs		1(-)	1(-)	1(-)
B105	Door		6(4)	6(4)	6(4)
B106	Small window		2(2)	2(2)	2(2)
B107	Medium window		7(0)	7(0)	7(0)
B108	Large window		3(0)	3(0)	3(0)
B109	Very large window	per unit	1(0)	1(0)	1(0)
B110	Office chair		2(-)	2(-)	2(-)
B111	Basic chair		12(-)	12(-)	12(-)
B112	Armchair		4(-)	4(-)	4(-)
B113	Oven with cooker		2(-)	2(-)	2(-)
B114	Fridge		2(-)	2(-)	2(-)
B115	Washing machine		2(-)	2(-)	2(-)



Table 2: Mean quantities for the damageable PSD-sensitive structural components of the case study RC building in X (Y) direction.

ID	Component	Unit	Quantity per storey		
			Storey 1	Storey 2	Storey 3
A101	Exterior beam-column joint (end-hooks)	per unit	4(-)	4(-)	4(-)
A102	Interior beam-column joint (weak columns)		6(4)	6(4)	6(4)
A103	Gravity column		6(-)	6(-)	6(-)

Table 3: Mean quantities for the damageable PFA-sensitive non-directional non-structural components of the case-study RC building.

ID	Component	Above EDP	Unit	Quantity per storey			
				Storey 1	Storey 2	Storey 3	
C101	Fancoil	1	per unit	8	8	8	
C102	Ceiling systems		per m <sup>2</sup>	418.5	418.5	432	
C103	Lighting systems		20	20	20		
C104	Piping systems – water distribution (pipe)		per 250m	0.879	0.879	0.879	
C105	Piping systems – heating distribution (pipe)		0.927	0.927	0.927		
C106	Sanitary waste piping		0.879	0.879	0.879		
C107	Small bookshelf		2	2	2		
C108	Large bookshelf		2	2	2		
C109	Luxurious bookshelf		2	2	2		
C110	Small wardrobe		2	2	2		
C111	Medium wardrobe		4	4	4		
C112	Large wardrobe		2	2	2		
C113	Small sofa		1	1	1		
C114	Medium sofa		per unit	3	3	3	
C115	Small table		6	6	6		
C116	Medium table		2	2	2		
C117	3 compartment shelves		6	6	6		
C118	4 compartment shelves		3	3	3		
C119	5 compartment shelves		2	2	2		
C120	Singe bed		2	2	2		
C121	Double bed		4	4	4		
C122	Kitchen equipment		2	2	2		
C123	Computers and notebooks		0	8	8	8	
C124	TV equipment		4	4	4		
C125	Fire sprinklers water piping		1	per 250m	0.753	0.753	0.753
C126	Fire sprinklers drop		12	12	12		
C127	Distribution panel for fire sprinkler		1	1	1		
C128	Hydraulic elevator		0	per unit	1	0	0
C129	Battery rack		1	0	0		
C130	Battery charger		1	0	0		
C131	Distribution panel for the elevator		1	0	0		

Knowing the quantities at each storey, creating SLFs necessitates the definition of fragility and consequence functions for all components within the inventory. Table 4 to Table 6 summarise the damage descriptions, the sources for the function definitions and the fragility parameters for structural, PSD-sensitive and PFA-sensitive non-structural components, respectively. For the majority of the components, fragility and consequence functions were adopted from the available literature ([19], [30], [31]), while for the remaining components, mean repair costs were based on typical costs expected in Italy. To what pertains the fragility functions of the latter components, they were primarily tied to fragilities of other components. This is a correlation assumption between two components, even though it was not directly implemented. In the absence of fragility functions for some non-structural components, some assumptions were made using engineering judgment. While many components (e.g. doors, chairs, fridges, washing machines) were assumed damaged when the interior masonry partitions have reached collapse DS, others (e.g. windows) were assumed damaged when the exterior masonry walls have reached collapse DS, considering that collapse of walls or partitions would damage the adjacent chairs, doors and windows. Similarly, TV and computers were considered damaged once there was 30% damage and falling of ceiling tiles and many other components (e.g. bookshelves, wardrobes, sofas, tables, shelves, beds and kitchen equipment) were damaged once there was large leakage of piping systems.

Table 4: Fragility function parameters and repair costs for PSD-sensitive non-structural components.

ID	Damage states	Source	Fragility function parameters		Mean repair cost €
			Median (% for PSD, g for PFA)	Dispersion	
B101	DS1 Light cracking	Cardone & Perone [19]	0.10	0.5	62
	DS2 Extensive cracking		0.30	0.5	117
	DS3 Corner crushing		0.75	0.4	234
	DS4 Collapse		1.75	0.35	234
B102	DS1 Light cracking	Sassun <i>et al.</i> [31]	0.15	0.5	62
	DS2 Extensive cracking		0.40	0.5	117
	DS3 Collapse		1.00	0.4	234
B103	DS1 Operational	FEMA P-58 [32]	0.18	0.52	34
	DS2 Damage limitation		0.46	0.54	62
	DS3 Significant damage		1.05	0.4	1243
	DS4 Near collapse limit state		1.88	0.38	1243
B104	DS1 Non-structural damage	Personal judgment	0.50	0.6	918
	DS2 Structural damage		1.70	0.6	4852
	DS3 Loss of live load capacity		2.80	0.45	30097
B105			1.88	0.38	220
B106			1.75	0.35	134
B107			1.75	0.35	212
B108			1.75	0.35	298
B109			1.75	0.35	449
B110	DS1 Damaged		1.88	0.38	199
B111			1.88	0.38	49
B112			1.88	0.38	199
B113			1.88	0.38	569
B114			1.88	0.38	649
B115			1.88	0.38	349

Table 5: Fragility function parameters and repair costs for PFA-sensitive non-structural components.

ID	Damage states	Source	Fragility function parameters		Mean repair cost €
			Median (% for PSD, g for PFA)	Dispersion	
C101	DS1 Falls		0.80	0.4	1035
	DS1 5% damaged		0.55	0.4	49
C102	DS2 30% damaged		1.00	0.4	69
	DS3 50% damaged		1.50	0.4	99
C103	DS1 Disassembly of rod system at connections	FEMA P-58 [32]	1.00	0.4	583
C104	DS1 Small leakage		0.55	0.4	307
	DS2 Large leakage		1.10	0.4	2302
C105	DS1 Isolated support fail- ure		0.55	0.4	307
			1.10	0.4	2302
C106	DS2 Multiple supports failure		1.20	0.4	525
			2.40	0.4	3737
C107					35
C108					80
C109					140
C110					70
C111					126
C112					199
C113					179
C114					399
C115	DS1 Damaged	Personal judge- ment	1.10	0.4	20
C116					
C117					80
C118					90
C119					99
C120					169
C121					349
C122					962
C123					1220
C124			1.00	0.4	610
C125	DS1 Spraying and drip- ping leakage		1.10	0.4	252
			2.40	0.5	1911
C126	DS2 Joints break – major leakage		0.75	0.4	43
			0.95	0.4	43
C127	DS1 Damaged	FEMA P-58 [32]	3.05	0.4	7298
C128	DS1 Damaged		0.50	0.3	10753
C129	DS1 Batteries spill acid		1.11	0.6	10032
C130	DS1 Damaged		1.07	0.4	9560
C131	DS1 Anchorage failure		3.05	0.4	7298

Consideration was already given here for correlations among damage states of different components in the case study building. Components like doors, windows, chairs were tied to the DS of causation component due to the absence of fragility functions in the literature. However, additional logical correlations based on engineering judgment were assigned among other components within the same EDP-sensitivity group.

Table 7 describes the damage of the causation component, as well as its effect on the correlated component. It is important to note that this set of correlations will not be considered within the component-based loss assessment framework hence some difference in results should be expected a priori should this aspect have a notable impact. However, a demonstration

of variation of including such correlations with respect to ignoring them in an SLF-based approach will be commented on later.

Table 6: Fragility function parameters and repair costs for structural components.

ID	Damage states	Source	Fragility function parameters		Mean repair cost €
			Median (% for PSD, g for PFA)	Dispersion	
A101	DS1 Light cracking	FEMA P-58 [32] for fragility func- tions and Cardone [33] for costs	2.00	0.4	2090
A102	DS2 Concrete spalling		2.75	0.3	3026
A103	DS3 Concrete crushing		5.00	0.3	4093
					1744
					2861
					4488

Table 7: Correlations between DSs component of the case study building.

Causation Component ID	Damage de- scription of causation component	Dependant Component ID	Effect on the dependent component	DS of a de- pendent component
C104	DS1 Small leakage	C102	30% damaged	DS2
		C103	Disassembly of rod system at connec- tions	DS1

## 4 RESULTS

The toolbox was applied at each storey of the building and SLFs were derived based on the component data provided previously. Correlations among dependent component DSs were considered as described in

Table 7. For PSD-sensitive components, a set of three SLFs were derived for both principal directions and the non-directional components, corresponding to each of the three storeys of the building. For PFA-sensitive components, loss functions for four floors were derived, based on whether the component was sensitive to the PFA of the above floor or the floor upon which it is placed. The PACT software [32] provided with FEMA P-58 was used to conduct the component-based loss estimation, where a non-directional conversion factor was assumed to be 1.2. Apart from record-to-record variability, no epistemic uncertainty was considered for simplicity, as this study acts as a comparative study between two methodologies.

To attain the SLFs, performance grouping was applied and Equation 2 was used to carry out regression and identify mean curves. Sample SLFs for the 2<sup>nd</sup> storey and 2<sup>nd</sup> floor of the building are provided in Figure 6 and regression parameters are provided in Table 8. Losses of non-structural (NS) components start accumulating at low values of PSD, which is particularly due to low capacities of interior and exterior infills (Table 4). In contrast, losses of structural (S) components start accumulating once a certain threshold of PSD value is reached, which could be attributed to the high capacities of well-designed ductile columns. The toolbox was also applied assuming component correlations. Figure 6(b) demonstrates the SLFs of PFA-sensitive components on the 2<sup>nd</sup> floor of the case study building. The consideration of correlation among some of the components as detailed in Table 7, has an impact on the losses within PFA values of 0.5 to 2.5g. The inclusion of correlations results in an increase in vulnerability through the curves shifting to the left in Figure 6(b).

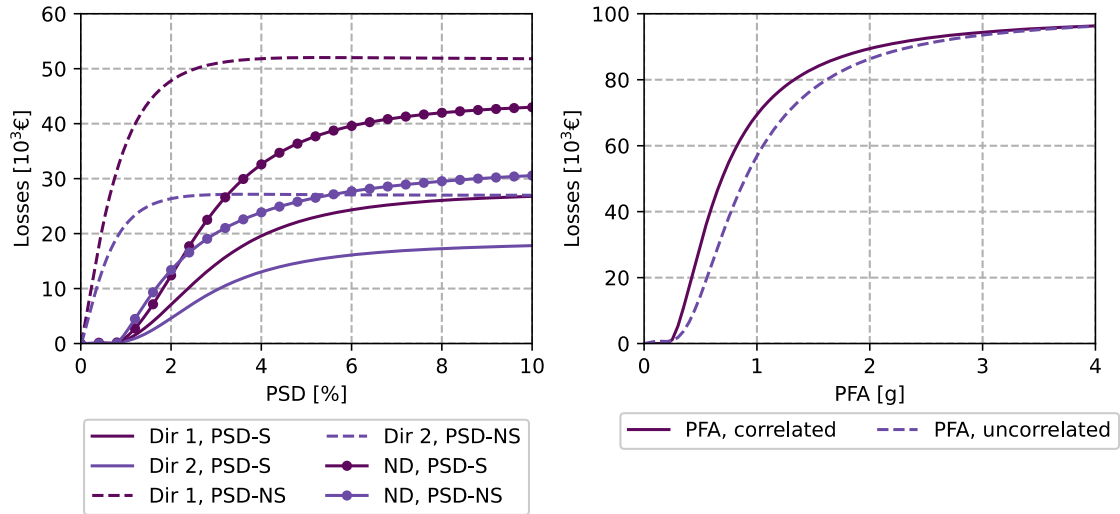


Figure 6: SLFs for the case-study building intermediate (2<sup>nd</sup>) storey level and 2<sup>nd</sup> floor (Equation 2). (a) PSD-sensitive components, (b) PFA-sensitive non-structural components.

Table 8: Regression parameters for the fitted SLFs at the 2<sup>nd</sup> storey of the case study building using Equation 2.

Performance group	Direction 1					Direction 2				
	$\alpha$	$\beta$	$\gamma$	$\delta$	$\varepsilon$	$\alpha$	$\beta$	$\gamma$	$\delta$	$\varepsilon$
PSD S	2.435	2.285	5.300	0.970	1.333	2.020	1.676	2.936	0.978	2.168
PSD NS	1.348	1.892	1.351	1.908	138.3	1.402	1.563	1.406	1.574	174.7
PFA NS, correlated	2.003	0.271	2.010	0.270	176.7	-	-	-	-	-
PFA NS, uncorrelated	2.112	0.410	2.115	0.408	259.7	-	-	-	-	-

Probabilistic seismic hazard analysis (PSHA) was performed using OpenQuake [34] with the SHARE hazard model [35]. A set of 30 ground motion record pairs were selected from the NGA West-2 database [36] with each record's soil type being consistent with that of the site. Hazard curves obtained from PSHA were used to carry out the loss assessment. Figure 7 illustrates the hazard curve for the selected case study location. The intensity measure (IM) selected was the spectral acceleration,  $Sa(T^*)$ , at a conditioning period,  $T^*$ . Since the building has two principal modes of vibration in two orthogonal directions, following the suggestion of FEMA P58 [5], a  $T^*$  of 1.1s corresponding to the arithmetic mean of two orthogonal modal periods was selected. Non-linear response-history analyses were conducted and the results were used to carry out loss assessment using the PACT software for a component-based approach and using the SLFs generated via the proposed toolbox for the SLF-based approach.

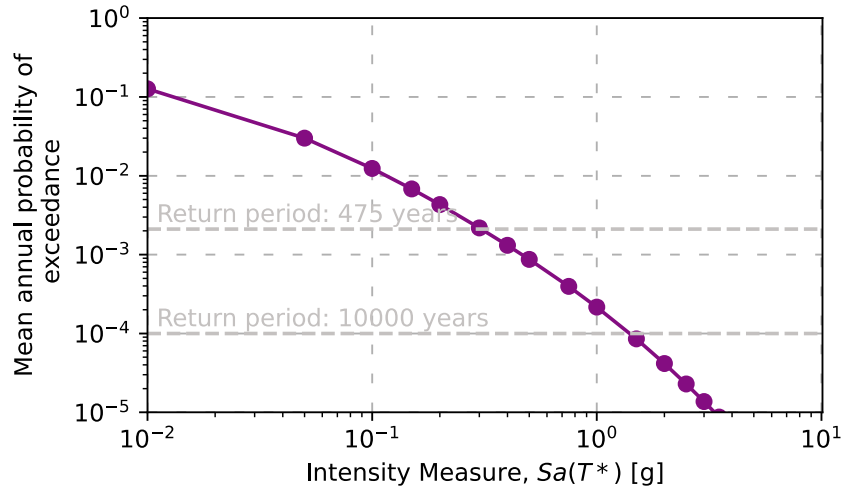


Figure 7: Hazard curve for the site considered in L'Aquila, Italy at a period of 1.1s.

The approach proposed by Ramirez and Miranda [37] was used to perform an SLF-based loss assessment. Residual deformations are accounted for to compute the probability of the building being demolished after an earthquake. The economic loss computed consists of the following terms: losses due to building collapsing; repair costs due to the building's structural and non-structural components being damaged; and losses resulting from the demolition of the building if excessive residual drifts were recorded. For the case-study building, probability of the building being demolished due to excessive residual drifts is assumed to be lognormally distributed with a median of 0.015 and a logarithmic standard deviation of 0.3 [37].

Based on the loss assessment results, the expected annual loss (EAL) was computed for the case study building by integrating the vulnerability curve, expressed in terms of expected direct economic loss as a function of IM, with the site hazard curve defined according to Equation 3.

$$EAL = \int E[L_r | IM] \left| \frac{dH}{dIM} \right| dIM \quad (3)$$

where  $dH/dIM$  is the mean annual frequency of the ground motion IM. EAL disaggregated by cost type and vulnerability curves are presented in Figure 8. The EAL computed using SLFs was 0.63%, which is slightly lower when compared to the one computed via the FEMA P-58 component-based approach, which amounted to 0.66%. As observed, the main contribution to the EAL comes from non-structural components, while structural components represent the lowest proportion. This demonstrates how structural components designed following seismic code provisions have larger capacities against damage. The similarity of vulnerability curves, as well as the proportions of contributions towards EAL, enforce the quality of a more simplistic SLF-based approach in ensuring proper assessment of losses when compared to the more rigorous component-based approach.

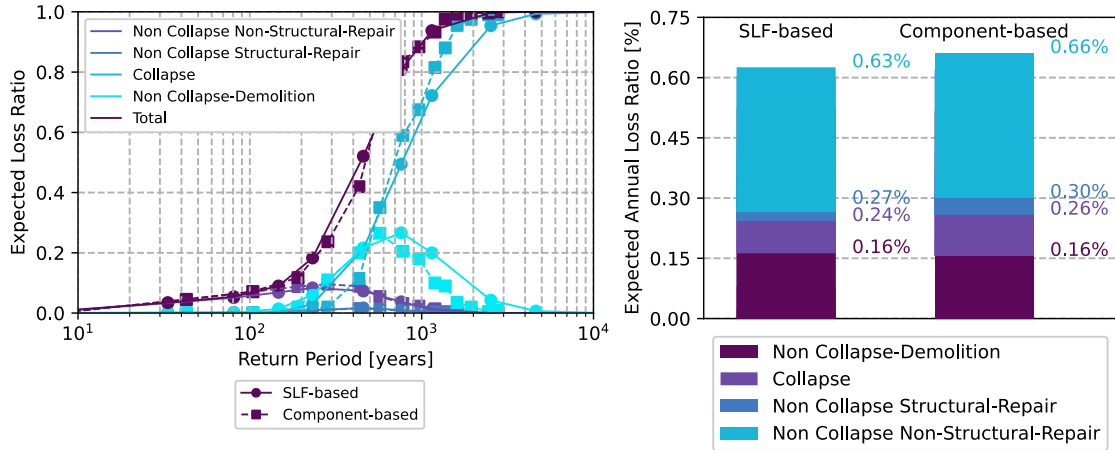


Figure 8: (left) Vulnerability curves and (right) expected annual loss showing the breakdown of different contributors in a comparative assessment between an SLF-based and component-based loss assessment approach.

Finally, Figure 9 provides the relative contributions to the vulnerability curves as a function of the return period. As observed, the main contributors at low hazard levels are the non-structural repair costs. With increasing return period, the costs from collapse and demolition start increasing, with collapse taking a significant portion of the costs at higher return periods. Cost contributions from demolition losses are quite high at high return periods, where in the absence of collapse the building needs to be demolished. Essentially, even though one might expect for structural component repair costs to increase with increasing return period, as they undergo damage, it precedes by the building needing demolition or collapse, therefore loss contributions from structural repair costs are inexistent at higher return periods as well.

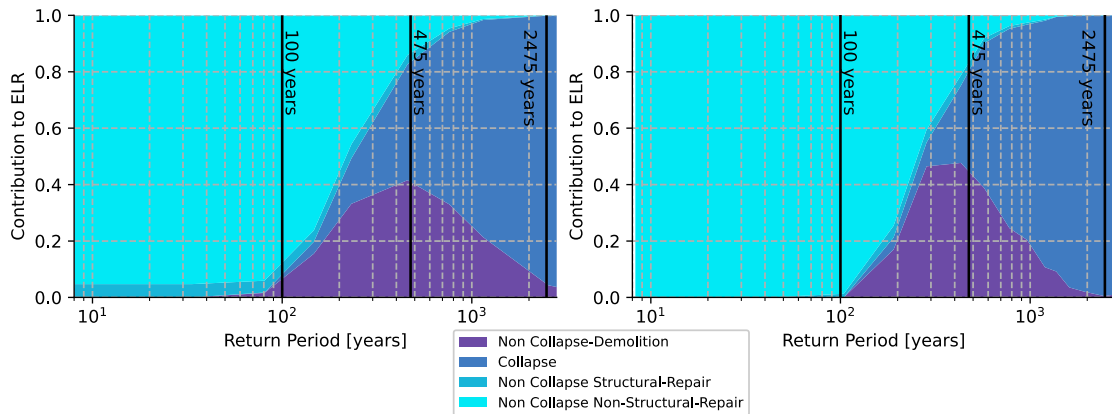


Figure 9: Relative contribution to expected loss with respect to increasing return period for a (left) SLF-based approach and (right) component-based approach. As reference points, the 100, 475 and 2475-year return periods have been annotated on each plot.

## 5 SUMMARY AND CONCLUSIONS

With the lack of available tools to develop storey loss functions (SLFs) to fit specific needs, this article aims to fill the gap by introducing an SLF generation toolbox for seismic design and assessment of buildings. A description of the toolbox is presented, and it was validated through an application to a case study building in a comparative study with the more rigorous component-based loss assessment described in FEMA P-58. Additionally, the toolbox was

applied to compare the effects of assumptions where component damage states were considered independent and where the dependency of damage states of different components was assumed. The main observations from the study are as follows:

- The toolbox can consider component correlations. An example at the 2<sup>nd</sup> floor of the building considering peak floor acceleration sensitive components demonstrated that inclusion of dependencies and interactions of various components may impact the vulnerabilities avoiding potential underestimations in costs;
- SLFs were developed for the entire case study reinforced concrete building accounting for the response in both directions and a subsequent loss assessment was carried out. Results were compared to a component-based loss assessment approach with a good match in EAL between the two approaches;
- A close match of SLF-based loss estimates to the detailed component-based loss assessment was observed in the distribution of losses among performance groups per intensity highlighting the validity of the developed tool and its accurate applicability for the intended scopes initially outlined;
- While important for loss assessment on existing buildings, the SLF generation toolbox may be even more of an important tool for new designs within new risk-based design approaches.

## ACKNOWLEDGEMENTS

The work presented in this paper has been developed within the framework of the project “Dipartimenti di Eccellenza”, funded by the Italian Ministry of Education, University and Research at IUSS Pavia.

## REFERENCES

- [1] ASCE 7-16, “Minimum Design Loads for Buildings and Other Structures,” Reston, VA, USA, 2016.
- [2] CEN, *Eurocode 8: design of structures for earthquake resistance, Part 1, General Rules, Seismic Actions and Rules for Buildings*. Brussels, Belgium: European Committee for Standardization (CEN), 2004.
- [3] NZS 1170.5:2004, *Structural design actions part 5: Earthquake actions*. Wellington, New Zealand, 2004.
- [4] K. A. Porter, “An Overview of PEER’s Performance-Based Earthquake Engineering Methodology,” *9th Int. Conf. Appl. Stat. Probab. Civ. Eng.*, vol. 273, no. 1995, pp. 973–980, 2003, doi: 10.1.1.538.4550.
- [5] FEMA, “FEMA P-58-1: Seismic Performance Assessment of Buildings: Volume 1 - Methodology,” Washington, DC, 2012.
- [6] M. Aschheim and E. F. Black, “Yield point spectra for seismic design and rehabilitation,” *Earthq. Spectra*, vol. 16, no. 2, pp. 317–335, May 2000, doi: 10.1193/1.1586115.
- [7] C. A. Cornell, “Calculating building seismic performance reliability: a basis for multi-level design norms,” in *11th World Conference on Earthquake Engineering*, 1996, p. 8.
- [8] R. C. Kennedy and S. A. Short, “Basis for seismic provisions of DOE-STD-1020,” Livermore, California, 1994.



- [9] H. Krawinkler, F. Zareian, R. A. Medina, and L. F. Ibarra, "Decision support for conceptual performance-based design," *Earthq. Eng. Struct. Dyn.*, vol. 35, no. 1, pp. 115–133, 2006, doi: 10.1002/eqe.536.
- [10] N. Luco, B. R. Ellingwood, R. O. Hamburger, J. D. Hooper, J. K. Kimball, and C. A. Kircher, "Risk-targeted versus current seismic design maps for the conterminous United States," 2007.
- [11] G. J. O'Reilly and G. M. Calvi, "Conceptual seismic design in performance-based earthquake engineering," *Earthq. Eng. Struct. Dyn.*, vol. 48, no. 4, pp. 389–411, Apr. 2019, doi: 10.1002/eqe.3141.
- [12] D. Vamvatsikos and M. A. Aschheim, "Performance-based seismic design via yield frequency spectra ‡," *Earthq. Eng. Struct. Dyn.*, vol. 45, no. 11, pp. 1759–1778, Sep. 2016, doi: 10.1002/eqe.2727.
- [13] J. Žižmond and M. Dolšek, "Formulation of risk - targeted seismic action for the force - based seismic design of structures," no. January, pp. 1–23, 2019, doi: 10.1002/eqe.3206.
- [14] D. Shahnazaryan and G. J. O'Reilly, "Integrating expected loss and collapse risk in performance-based seismic design of structures," *Bull. Earthq. Eng.*, vol. 19, no. 2, pp. 987–1025, Jan. 2021, doi: 10.1007/s10518-020-01003-x.
- [15] C. M. Ramirez and E. Miranda, "Building specific loss estimation methods & tools for simplified performance-based earthquake engineering," *Blume Cent. Rep.*, no. 171, 2009.
- [16] A. Silva, L. Macedo, R. Monteiro, and J. M. Castro, "Earthquake-induced loss assessment of steel buildings designed to Eurocode 8," *Eng. Struct.*, vol. 208, p. 110244, Apr. 2020, doi: 10.1016/j.engstruct.2020.110244.
- [17] A. N. Papadopoulos, D. Vamvatsikos, and A. Kazantzi, "Development and application of FEMA P-58 compatible story loss functions," *Earthq. Spectra*, vol. 35, no. 1, pp. 39–60, Feb. 2019, doi: 10.1193/020518EQS033M.
- [18] D. Ottonelli, S. Cattari, and S. Lagomarsino, "Displacement-Based Simplified Seismic Loss Assessment of Masonry Buildings," *J. Earthq. Eng.*, vol. 24, no. sup1, pp. 23–59, 2020, doi: 10.1080/13632469.2020.1755747.
- [19] D. Cardone and G. Perrone, "Developing fragility curves and loss functions for masonry infill walls," *Earthq. Struct.*, vol. 9, no. 1, pp. 257–279, 2015, doi: 10.12989/eas.2015.9.1.257.
- [20] A. Chiozzi and E. Miranda, "Fragility functions for masonry infill walls with in-plane loading," *Earthq. Eng. Struct. Dyn.*, vol. 46, no. 15, pp. 2831–2850, 2017, doi: 10.1002/eqe.2934.
- [21] C. Del Gaudio *et al.*, "Empirical fragility curves for masonry buildings after the 2009 L'Aquila, Italy, earthquake," *Bull. Earthq. Eng.*, vol. 17, no. 11, pp. 6301–6330, 2019, doi: 10.1007/s10518-019-00683-4.
- [22] G. Perrone, D. Cardone, G. J. O'Reilly, and T. J. Sullivan, "Developing a Direct Approach for Estimating Expected Annual Losses of Italian Buildings," *J. Earthq. Eng.*, vol. 00, no. 00, pp. 1–32, 2019, doi: 10.1080/13632469.2019.1657988.
- [23] T. J. Sullivan, "Use of Limit State Loss versus Intensity Models for Simplified Estimation of Expected Annual Loss," *J. Earthq. Eng.*, vol. 20, no. 6, pp. 954–974, 2016, doi: 10.1080/13632469.2015.1112325.

- [24] G. J. O'Reilly, T. J. Sullivan, and A. Filiatrault, "Implications of a More Refined Damage Estimation Approach in the Assessment of RC Frames," *16th World Conf. Earthq. Eng.*, no. February, 2017.
- [25] W. Carofilis, G. Gabbianelli, and R. Monteiro, "Assessment of Multi-Criteria Evaluation Procedures for Identification of Optimal Seismic Retrofitting Strategies for Existing RC Buildings," *J. Earthq. Eng. In-press*, vol. 00, no. 00, pp. 1–34, 2021, doi: 10.1080/13632469.2021.1878074.
- [26] CEN, *EC. EN 1992-1-1 Eurocode 2: Design of concrete structures - Part 1-1: General rules and rules for buildings*. Brussels. Brussels, Belgium: European Committee for Standardization (CEN), 2004.
- [27] CEN, "Eurocode 8: Design of Structures for Earthquake Resistance - Part 1: General Rules, Seismic Actions and Rules for Buildings (EN 1998-1:2004)," Brussels, Belgium, Comité Européen de Normalisation, 2004.
- [28] S. Mazzoni, F. Mckenna, M. H. Scott, and G. L. Fenves, "OpenSees Command Language Manual," 2006.
- [29] D. Vamvatsikos and C. A. Cornell, "Applied incremental dynamic analysis," *Earthq. Spectra*, vol. 20, no. 2, pp. 523–553, 2004, doi: 10.1193/1.1737737.
- [30] Applied Technology Council, "FEMA P-58-2: Seismic Performance Assessment of Buildings. Volume 2 – Implementation Guide," *Fema P-58*, vol. 2, no. December 2018, p. 378, 2018, [Online]. Available: <https://www.fema.gov/media-library/assets/documents/90380>.
- [31] K. Sassun, T. J. Sullivan, P. Morandi, and D. Cardone, "Characterising the in-plane seismic performance of infill masonry," *Bull. New Zeal. Soc. Earthq. Eng.*, vol. 49, no. 1, pp. 98–115, 2016, doi: 10.5459/bnzsee.49.1.98-115.
- [32] FEMA, "FEMA P58-3. Seismic Performance Assessment of Buildings Volume 3 - Performance Assessment Calculation Tool (PACT)," Washington, D.C., 2012.
- [33] D. Cardone, "Fragility curves and loss functions for RC structural components with smooth rebars," *Earthq. Struct.*, vol. 10, no. 5, pp. 1181–1212, 2016, doi: 10.12989/eas.2016.10.5.1181.
- [34] M. Pagani *et al.*, "OpenQuake Engine : An Open Hazard ( and Risk ) Software for the Global Earthquake Model," no. September, 2014, doi: 10.1785/0220130087.
- [35] R. W. Musson *et al.*, "The 2013 European Seismic Hazard Model: key components and results," *Bull. Earthq. Eng.*, vol. 13, no. 12, pp. 3553–3596, 2015, doi: 10.1007/s10518-015-9795-1.
- [36] T. D. Ancheta *et al.*, "NGA-West2 database," *Earthq. Spectra*, vol. 30, no. 3, pp. 989–1005, 2014, doi: 10.1193/070913EQS197M.
- [37] C. M. Ramirez and E. Miranda, "Significance of residual drifts in building earthquake loss estimation," *Earthquake Engineering and Structural Dynamics*, vol. 41, no. 11, pp. 1477–1493, 2012, doi: 10.1002/eqe.2217.